Supplementary Data

Supplementary Figure 1. Experimental workflow for detecting and prioritising sequence variants, and validation of MCD-related genes.

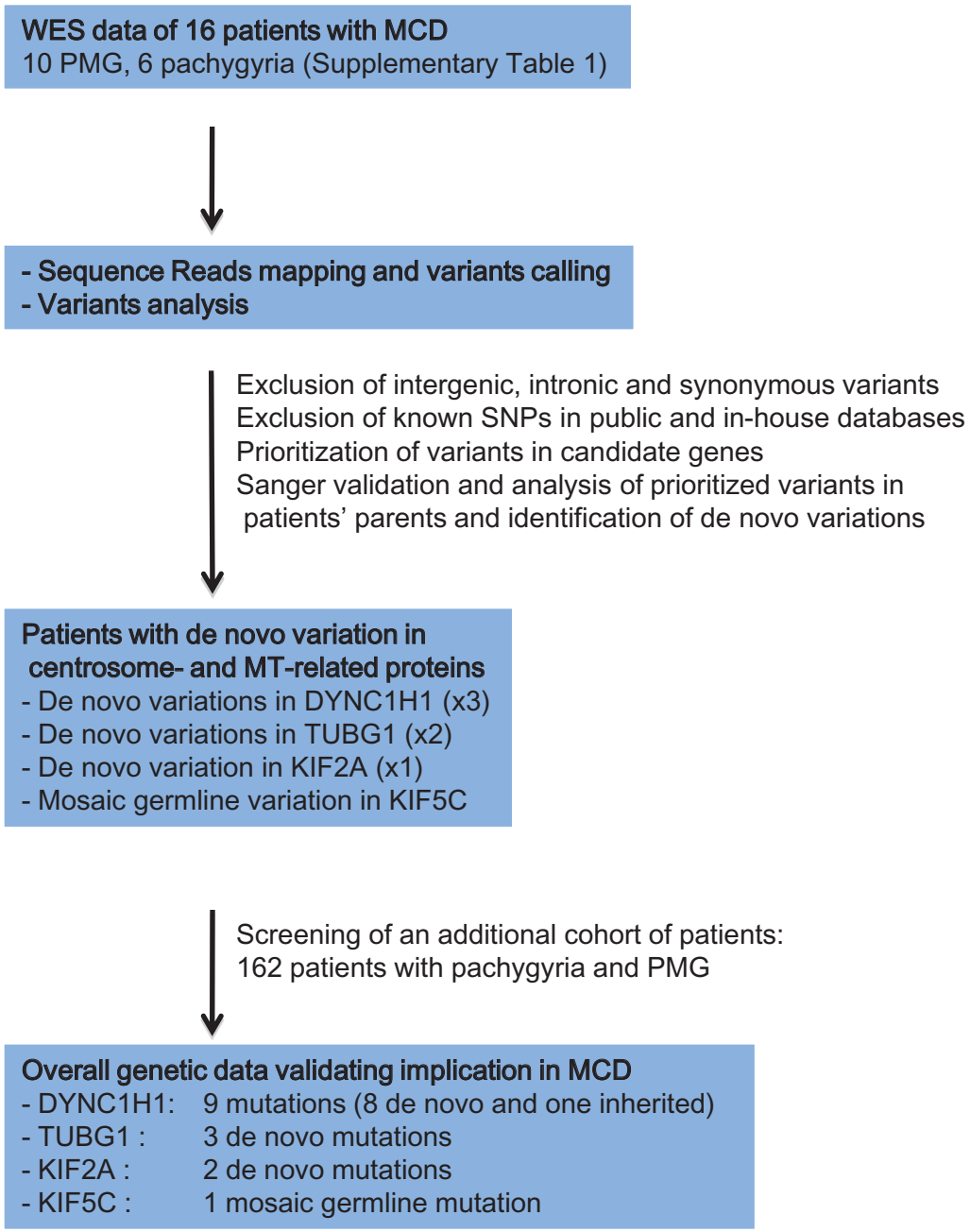

Supplementary Figure 1

Supplementary Figure 2. Genetic analysis of the P20 family

(a) Pedigree of the P20 family. Solid symbols represent affected individuals; central dots represent obligate carrier individuals. The III.3 subject was chosen to undergo exome sequencing. (b) X chromosome genotyping of P20 family members. Note that this analysis excludes X-linked transmission of the pathology. (c) Linkage analysis (with lod score value) for chromosome SNPs showing the non-excluded interval of 44.5Mb (with a lod score of 0.9). (d) Haplotypes neighboring *KIF5C* for II.3, III.4 and III.5 individuals. This reveals the transmission of the same haplotype from the mother to the two brothers (III.4 (affected) and III.5 (unaffected)), reinforcing the hypothesis of transmission of a germline mosaic mutation in *KIF5C* (M: mutated KIF5C; N: normal KIF5C) (e) chromatograms for P20 individuals showing normal and mutated sequences of *KIF5C.* Note the co-segregation of the mutation with the phenotype.

a

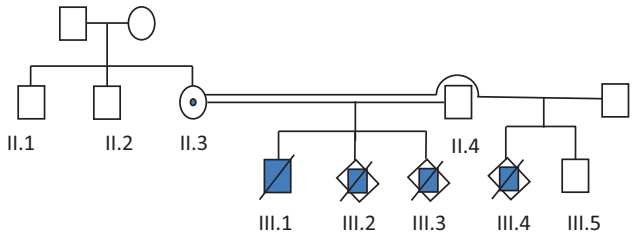

b

	II.3		III.1	III.2	III.3	III.4	III.5
DXS1060	243	249	243	243	243	243	243
DXS1223	159	151	159	159	159	159	159
DXS8051	124	120	124	124	124	124	124
DXS7108	252	252	252	252	252	252	252
DXS1224	164	164	164	164	164	164	164
DXS987	215	209	209	215	215	215	215
DXS1226	296	286	286	296	296	296	286
DXS1214	292	292	292	292	292	292	292
DXS1068	254	262	262	254	262	254	262
DXS993	287	270	270	287	270	287	270
DXS991	333	327	327	333	327	333	327
DXS986	166	166	166	166	166	166	166
DXS990	126	126	126	126	126	126	126
DXS1106	128	130	130	128	130	128	130
DXS8055	317	315	315	317	315	317	317
DXS1001	199	208	208	199	208	199	199
DXS1047	168	162	162	168	162	168	168
DXS1227	82	90	90	82	90	82	90
DXS8043	161	159	161	161	159	161	159
DXS998	119	117	119	119	117	119	117
DXS8091	89	71	89	89	71	89	71
DXS8069	140	142	140	140	142	140	142
DXS1073	308	310	308	308	308	310	310

Excluded region

non informative region

c

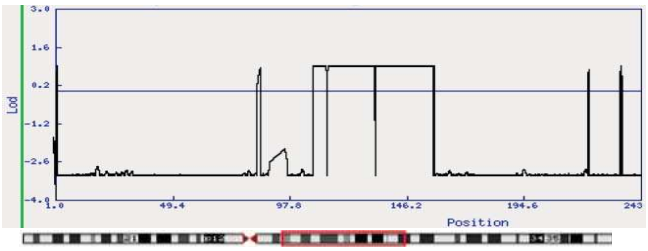

d

		II.3		III.4		III.5	
D2S112	133,12Mb	163	165	163	161	163	157
D2S151	147,78Mb	237	239	237	237	237	241
KIF5C	**149,63-149,88Mb**	N	N	M	N	N	N
D2S2241	154,51Mb	93	97	93	93	93	97
D2S142	156,28Mb	274	268	274	276	274	274

e

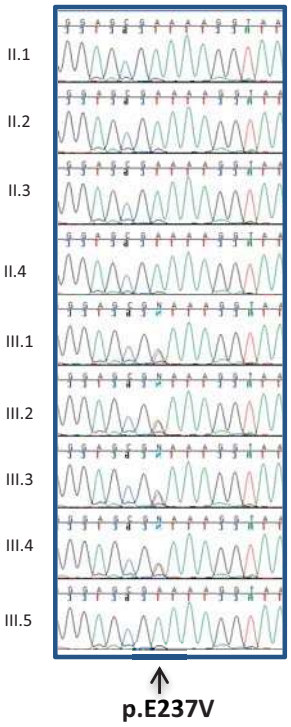

Supplementary Figure 2

Supplementary Figure 3. Functional consequences, expression and sublocalization of the p.E237V *KIF5C* mutation.

(a) Allelic expression of *KIF5C* in lung and brain tissues from the fetus-III.4 of P20 family. Primers hsKIF5C-3F TGCGTATGGGCAGACTTCATCAGGA and hsKIF5C-10R CCGAGTCATCTTGCTGTCCCGGT were used to perform RT-PCR experiments. These primers correspond to sequences that are located in exons 3 and 10 (separated by a distance of 120 kb) and allowed the amplification of a 610 bp cDNA fragment. Electrophoregrams show cDNA sequences around the mutations and illustrate expression of both alleles in these tissues. Note that these results indicate that KIF5C is not imprinted (at least in these two tissues). (b) Expression and purification of recombinant wild type and p.E237V mutant KIF5C proteins containing the motor domain, neck domain and a portion of the coiled-coil stalk. C-terminally His_6-tagged sequences encoding AA 1-380 of KIF5C were cloned into the pET23b vector and the recombinant proteins expressed in *E. coli* BL21 DE3 pLysS. Each protein was purified from soluble extracts of the host cells by affinity selection on a column of Co^{++}-bound agarose, and the purity of the product assessed by SDS-PAGE. Left hand tracks, total soluble protein extracts; right hand tracks, affinity purified proteins. (c) Recombinant KIF5C proteins behave as dimers. Purified recombinant wild type and mutant (p.E237V) form of KIF5C were analyzed by gel filtration on Superose 6. Note that relative to globular marker proteins (arrowed: thyroglobulin [black; 670kDa], IgG [orange; 158kDa], ovalbumin [purple; 44kDa], myoglobin [red; 17kDa]) both recombinant proteins migrate at a position consistent with their existence as dimers associated via their content of coiled-coil stalk domain. (d) MRI of the III.1 Patient from the P20 family. Axial T1 and T2 weighted images performed at 5 days of life show frontal and perisylvian coarse polymicrogyria. Sagittal T1-weighted section shows thin corpus callosum with normal brainstem and cerebellar vermis.

Briefly, the proband (Patient III.1) was the second child of non-consanguineous parents. Intrauterine growth retardation, severe arthrogryposis and microcephaly (-4 SD) were noted at birth. Clonic seizures started during the first months of life, controlled with carbamazepine. Brain MRI performed at 7 days showed a thin cortex with irregularly bumpy sulci and an irregular interface between the cortex and white matter over both frontal regions. We considered these MRI features to be compatible with a diagnosis of PMG. Subsequently, the mother had 3 medical abortions (around 23 GW) for male foetuses that showed developmental delay and

foetal akinesia. Anatomical and histological analyses suggested the presence of malformations that included diffuse polymicrogyria, gyral simplification, delayed development of the cerebellum and brainstem and abnormal positioning of the corticospinal tracts.

(e) Subcellular localization of human wild type and mutant KIF5C (p.E237V) in fibroblasts transfected with promotor-driven cDNA constructs. Note that the p.E237V mutated KIF5C protein (green) co-localises with and decorates MT's (identified by the a-tubulin antibody and revealed in red) but does not appears as cytoplasmic puncta as does the WT KIF5C protein. Scale bar: 20μm

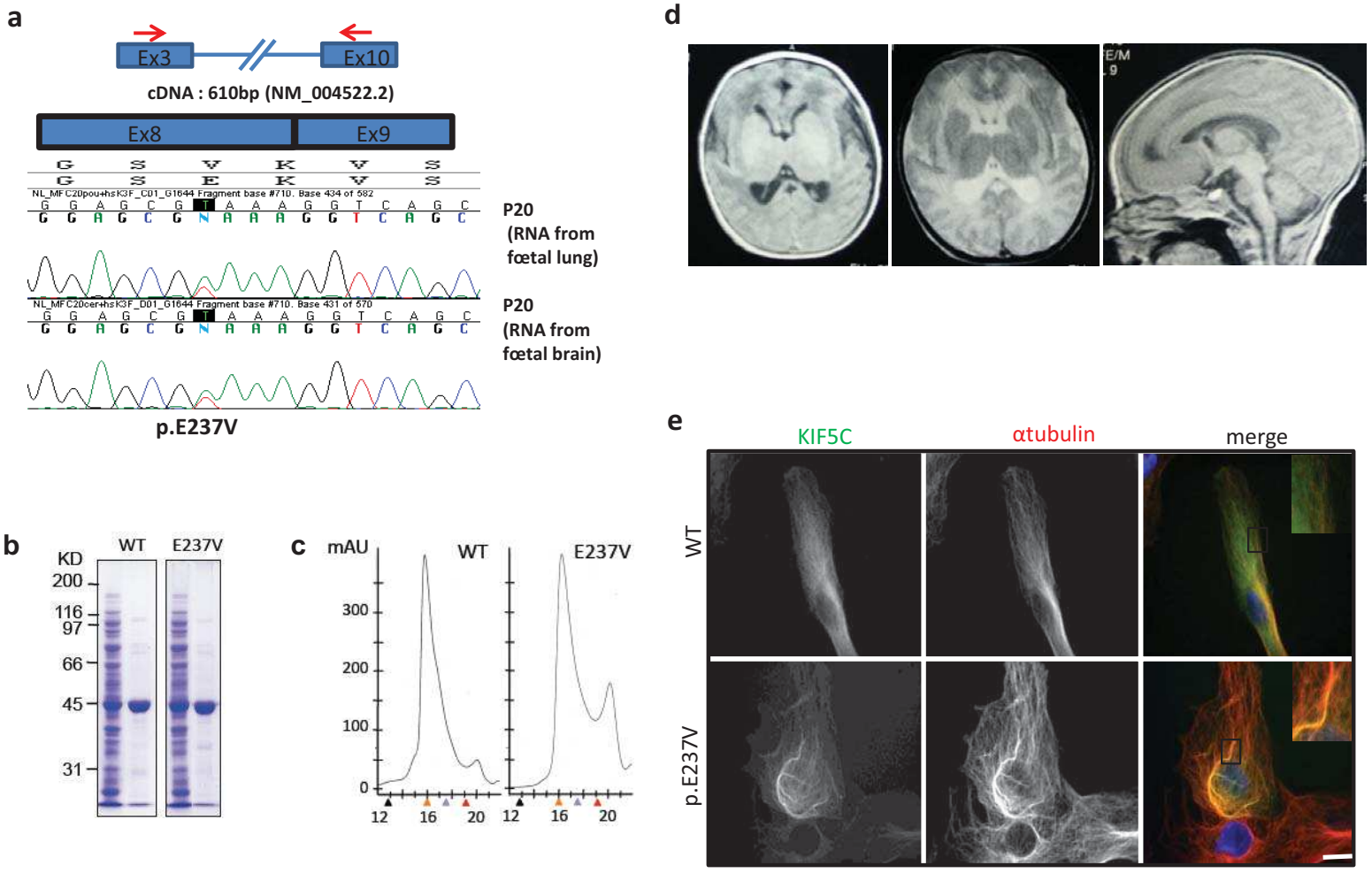

Supplementary Figure3

Supplementary Figure 4. Expression and subcellular localization of KIF2A.

(a) Subcellular localization of wild type and mutant KIF2As (green) in transfected fibroblasts. Note that both KIF2A mutants (p.S317N and p.H321D) co-localize with MTs (red) and are absent from the nucleus, while the KIF2A WT protein shows a diffuse cytoplasmic and nuclear pattern of expression. Centrosomal enrichment is observed in the case of both the WT and mutant KIF2A proteins. Scale bar: 20μm. (b) Allelic expression of KIF2A in fibroblasts derived from the patient with the p.H321D mutation. RT-PCR using hsKIF2A-9F (5-TGACTCAGCTCCTAATGAAATGGT-3) and hsKIF2A-17R (5-TCTGGTTTGGTGGATGGTGC-3) primers allows amplification of the KIF2A cDNA from exon 9 to 17. This reveals biallelic expression of KIF2A in the patient's fibroblasts, indicating that *KIF2A* is not imprinted in this tissue.

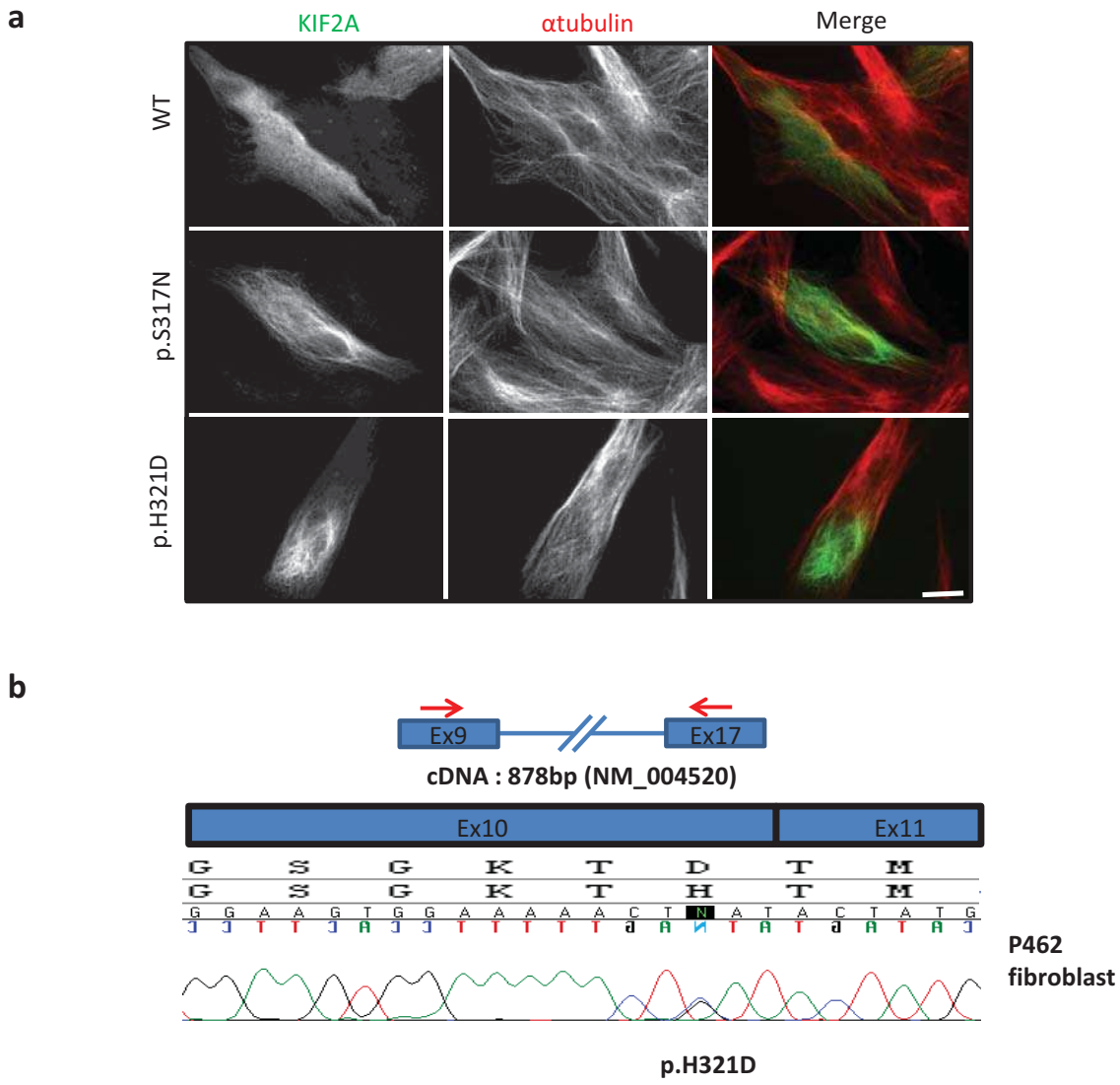

Supplementary Figure 4

Supplementary Figure 5. A dominant form of MCD is associated with the p.K3241T mutation in *DYNC1H1*.

(a) Pedigree of the 346D family. Solid symbols represent affected individuals. (b) Segregation of the *DYNC1H1* mutation in the family (c) Evolutionary conservation of the p.K3241 residue. (d) Axial MRI of the 346D family: mother (upper) and both children (bottom) respectively, showing the same pattern of posterior pachygyria with a thick cortex (asterisk) more pronounced in the two children compared with the less severely affected mother.

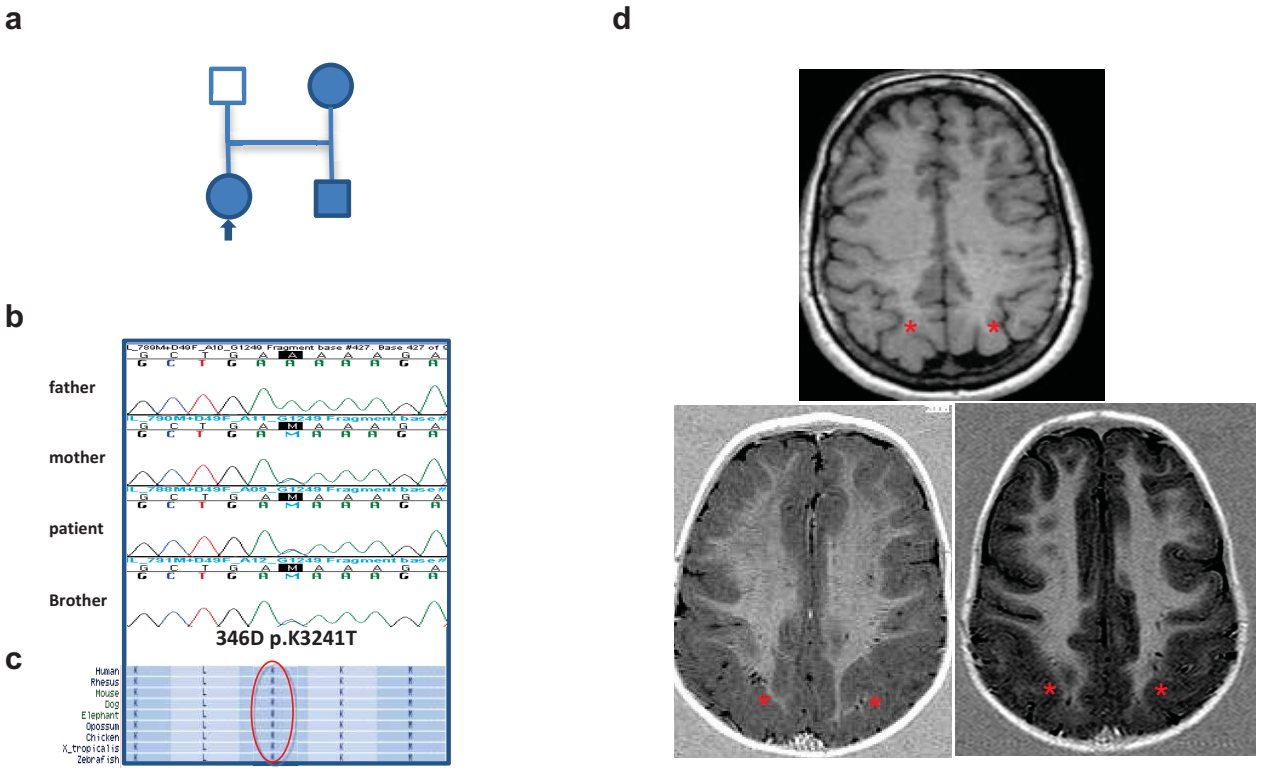

Supplementary Figure 5

Supplementary Figure 6. Effect of g-tubulin mutations on susceptibility to proteolysis in vitro

^{35}S-methionine-labelled products generated by transcription/translation in rabbit reticulocyte lysate were subjected to proteolysis by incubation with proteinase K as described by Tian et al.[1]. At the times shown (in minutes), aliquots were withdrawn, the reactions quenched by the addition of PMSF and the products analyzed by SDS-PAGE. FL, full-length g-tubulin. Note that the integrity of the recombinant proteins is not significantly affected by either of the disease-associated mutations.

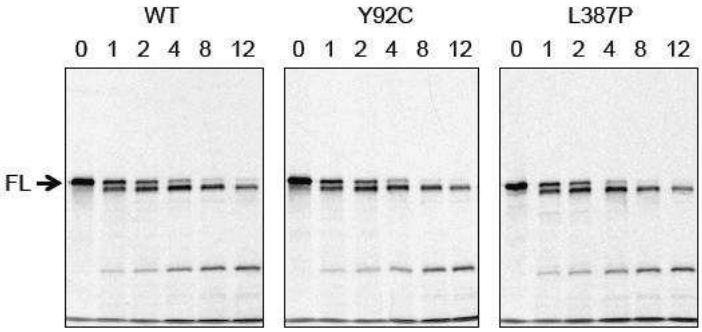

Supplementary Figure 6

Supplementary Figure 7. Analysis of the consequences of TUBG1 mutations in a yeast (S. cerevisiae) model

(a) Partial protein sequence of human TUBG1 in the region of p.Y92C and p.L387P aligned with *S. cerevisiae* Tub4p sequences. Yeast has a single g-tubulin gene (Tub4p), which shares 40 to 45% sequence identity with mammalian g-tubulin isotypes. Disease-associated residues are conserved but not identical: tyrosine (Y) at position 92 is replaced in yeast by tryptophan (W), while leucine (L) at position 387 is replaced in yeast by valine (V). To examine potential dominant effects of disease-associated mutations, we inserted p.W92C and p.V387P mutations into the yeast *Tub4* locus in heterozygous diploid strains. Three independent heterozygous diploids did not display growth defects on rich medium, establishing that all the mutant heterozygous strains were viable. p.V387P heterozygous diploids were recovered at the expected frequency (90%). In contrast, the p.W92C mutation seemed to be deleterious in that very few (10%) diploid mutants were obtained, showing that even in the heterozygous state the *tub4-W92C* mutation is toxic. However, analysis of mutant homozygotes revealed that the *tub4-W92C* mutation is viable (i.e. spores bearing the mutation were obtained at the expected frequency). *tub4-V387P* haploid spores were also viable when present as the sole copy of *Tub4*. (b) Merged Z stack images showing MTs in WT, p.W92C and p.V387P in budding yeast cells labeled with GFP-Tub1p (a-tubulin, green). Scale bar, 5 mm. To address MT organization in strains bearing the tub4-W92C and tub4-V387P mutations, we imaged cells using a-tubulin labeled with a TUB1::GFP fusion integrated at the *URA3* locus[2]. We found that the spindle pole body (SPB; the yeast equivalent of the centrosome) maintained its essential function. Indeed, for each mutation, MT's were nucleated from the SPB at each cell cycle. To investigate whether the γ-tubulin disease substitutions alter MT dynamics, MT number and/or stability, we examined MT+ end and astral MTs dynamics in living cells[3]. In order to analyse MT + ends dynamics we monitored G1 cell MT + ends labeled with Bik1p-GFP using time-lapse video microscopy. At least 30 MTs were analyzed and no significant differences were observed in tub4-W92C and tub4-V387P compared to wild type cells (Supplementary Table 6). These results suggest that MT + ends dynamics are unaffected in the g-tubulin mutants. We also examined astral MTs in living cells by monitoring dynamic astral MTs in G1 cells. GFP-Bik1p (an a-tubulin binding protein[4]) labeled MTs from heterozygous strains p.W92C and p.V387P were imaged. The p.W92C substitution resulted in

significant changes in measured MT parameters (Supplementary Table 7): we observed an overall enhancement of MT length in p.W92C cells (3.3 +/- 0.25 μm) compared to wild type cells (2.2 +/- 0.14 μm) and p.V387P cells (2.4 +/- 0.15 μm). In addition, the average maximal length of astral MTs also increased in tub4-W92C cells (4.8 +/- 0.33 μm) compared to wild type (3.1 +/- 0.19 μm) and V387P cells (3.3 +/- 0.19 μm), while more numerous MTs were observed in W92C cells (3.4 +/- 0.11 MT/Cell) compared to wild type (2.3 +/- 0.09 MT/cell) and V387P cells (2.5 +/- 0.07 MT/cell). Moreover, we found an effect of the tub4-W92C and tub4-V387P mutations on MT assembly: the frequency at which new MTs emanating from the SPBs became visible (i.e. nucleation or regrowth from existing microtubules) was significantly decreased in tub4-W92C cells (0.5 +/- 0.07 MTs assembled/min) relative to wild-type cells (1.42 +/- 0.11 MTs assembled/min; Supplementary Table 7). Thus, MT lengthening and an enhanced number in tub4-W92C cells is probably a consequence of MT nucleation in a manner that may increase overall polymer stability.

a

92

Human γ Tubulin Chain 1 L Y N P E N I Y L S E H G G G A G N N W A

Yeast Tub4p F F D P R N T W V A S D G A S A G N S W A

387

Human γ Tubulin Chain 1 N H T S I S S L F E R T C R Q Y D K L R K

Yeast Tub4p N M S T V V N V F E N A C N T F D K V E A

b

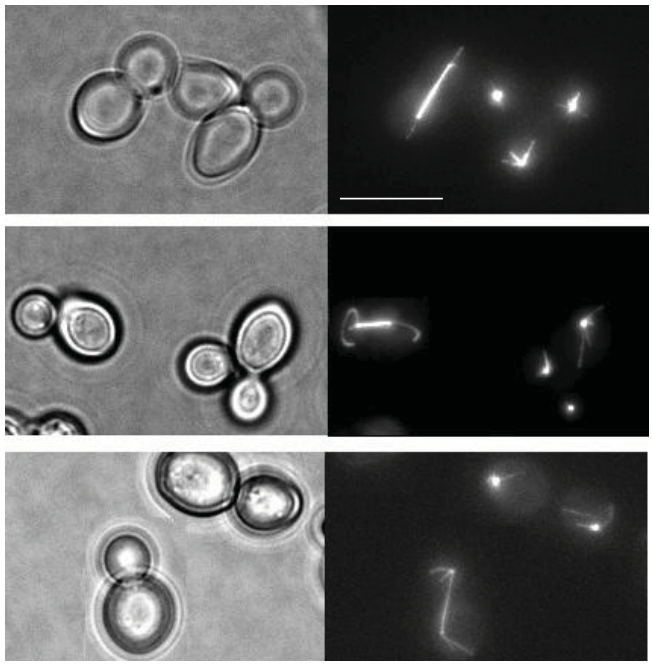

Supplementary Figure 7

Supplementary Figure 8. MT-dependent transport and MCD

Upper part: Schematic representation of cells in the ventricular zone (VZ), subventricular zone (SVZ), intermediate zone (IZ) and cortical plate (CP) corresponding respectively to progenitor proliferation, neuronal polarity, migration and differentiation steps. Bottom part (left): Representation of a mitotic cell during neuroblast proliferation steps in the VZ. KIF2A, TUBG1 and WDR62 are grouped in the spindle pole body, and KIF2A is also enriched in kinetochores structures. The LIS1/DYNC1H1 complex and TUBG1 proteins are distributed along mitotic spindle MTs with an additional localization of LIS1/DYNC1H1 at astral MT extremities. Bottom (right): Representation of the centrosome, MT and MT-motor protein complexes highlighting a functional coupling between centrosomal and MT-dependent transport proteins as illustrated by the location of MCD-related proteins (shown in red) in both structures. For simplicity, MT-dependent anterograde transport along MTs is shown in the Figure as mediated only by KIF5 and KIF1A. Interaction between KIF5 and LIS1/NDEL1 has been reported to be required for anterograde transport of the dynein-dynactin complex[5]. KIF1A has also been shown to interact with doublecortin (DCN) and mediates VAMP2 transport[6]. Loading and uploading of cargos is dependent on rabGTPases, molecular switches regulated by RabGAPs and RabGEFs, TBC1D22B (a RabGAP protein) is included in the illustration because of the identification of a *de novo* nonsense mutation in patient P386 (with diffuse PMG, Supplementary Table 8). Vesicle retrograde transport is mediated by cytoplasmic heavy chain dynein (DYNC1H1) when associated with dynactin and activated by LIS1/NDE1 or NDEL1 effectors. KIF2A is shown located at MT plus ends where it functions as a MT depolymerase.

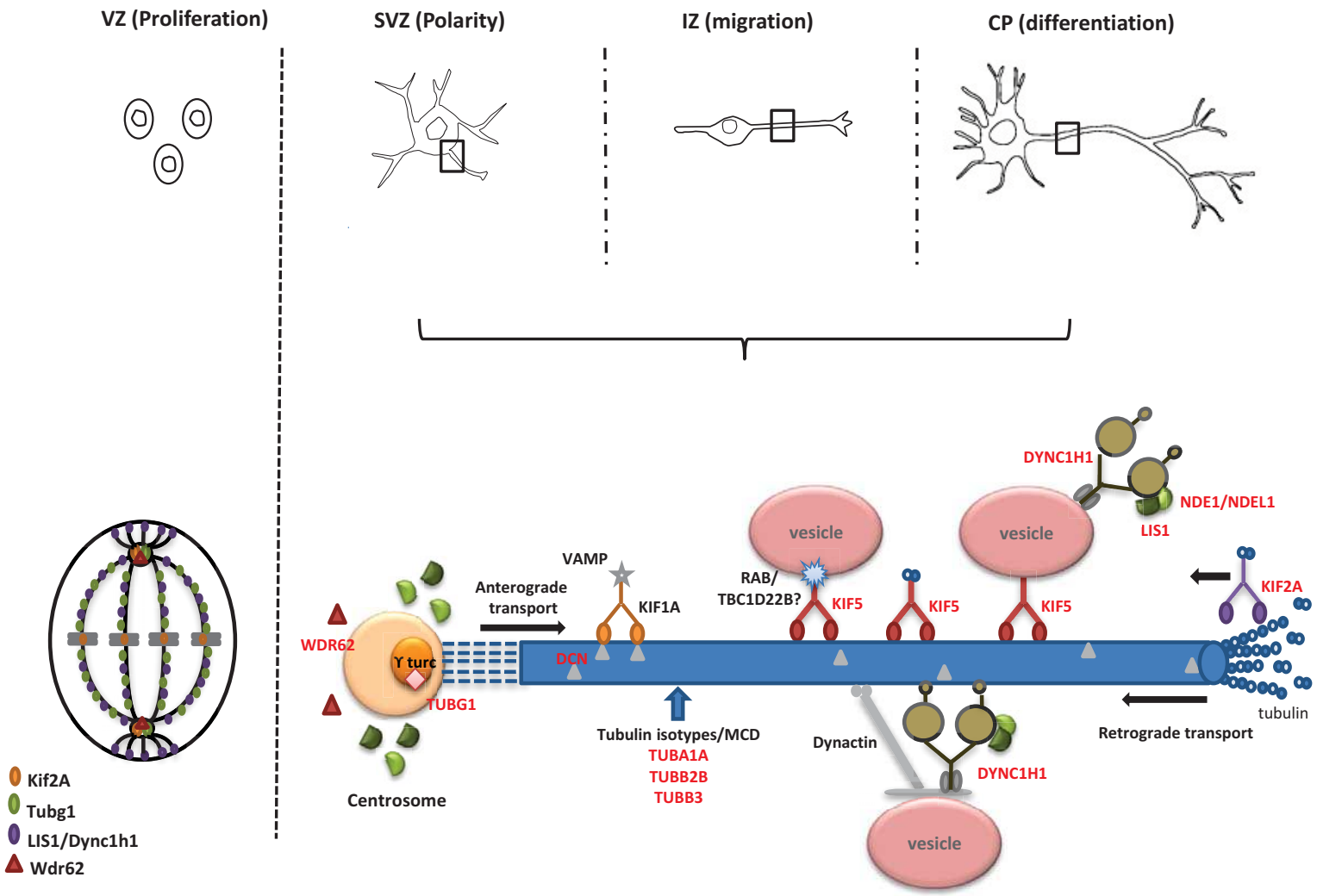

Supplementary Figure 8

Supplementary Table 1. Summary of the phenotype presented by individuals selected for exome sequencing.

Patients are grouped according to the classification proposed by Barkovich[7]. Brain MRI of patients of groups A and B exhibit polymicrogyria (PMG) or lissencephaly phenotypes, respectively. (MCD: malformation of cortical development; CC: corpus callosum; SD: standard deviation; SBH: subcortical band heterotopias; PMG: polymicrogyria; Y: yes; N: normal; F: familial; S: sporadic; post.: posterior.

Group	Patient	Microcephaly	MCD	Basal ganglia	Corpus Callosum	Brainstem	Cerebellum	Familial or sporadic
A	**P20**	(-4SD)	Frontal and perisylvian PMG	N	Thin	N	N	F
A	**P122**	(-4SD)	Post. Pachygyria - Frontal PMG	Dysmorphic	Dysmorphic	Hypoplasic	Vermian hypoplasia	S
A	**P205**	N	Asymetric Fronto-Parietal PMG	Dysmorphic	Post CC agenesis	Hypoplasic	Vermian hypoplasia	S
A	**P317**	N/A	Bifronto-perisylv Pmg	N	Thin	N	N	S
A	**P378**	(- 3SD)	Diffuse PMG	N	Thin	N	N	S
A	**P386**	(- 4SD)	Perisylvian PMG	N	N	Hypoplasic	N	S
A	**P348**	N	Perisylvian PMG	N	Thin	N	N	S
A	**P398**	N	Bifronto-perisylv PMG	N	Dysmorphic	N	N	S
A	**P425**	N	Gyral simplification	N	N	Hypoplasic	Hypoplasic	S
A	**P506**	N	Perisylvian PMG	N	Thin	N	N	S
B	**P217**	(-4SD)	Frontal PMG and perisylvian-post agyria	Dysmorphic	Thick and dysmorphic	Hypoplasic	Vermian hypoplasia	S
B	**P306**	(-2.5 DS)	Post. Agyria and frontal pachygyria	Dysmorphic	Thick and dysmorphic	Hypoplasic	N	S
B	**P351**	(-3SD)	Post. Agyria and frontal pachygyria	N	Thick and dysmorphic	Thin	Hypoplasic	S
B	**P367**	(-5.5SD)	Post. Agyria and frontal pachygyria	N	Thin	N	N	S
B	**P388**	(-4SD)	Post. Agyria and frontal pachygyria	N	Thick and dysmorphic	N	N	S
B	**P462**	(-4SD)	Frontal SBH and post. pachygyria	Dysmorphic	Thin	N	N	S

Supplementary Table 2. Exome sequencing data. For each patient's DNA the mean depth and % of nucleotides with a coverage depth of at least 5X or 15X, respectively, and the total number of detected variations are shown**.** WG: whole genome; Snp: single nucleotide polymorphism; del: deletion; dup: duplication; x/y: heterozygous/homozygous. Note that the same variant can be counted in different types of mutations because of the existence of multiple isoforms for some genes.

Group	Patient	Mean depth	>5X (%)	>15X (%)	Total variations	Total variations (excluding snp>1%	Essential splicing sites	Synonymous	Non-synonymous	In frame del or dup	Frameshift	Stop gain	Start or stop loose
A	**P20**	51	94	83	24058	613	38/2	137/9	403/12	3/0	7/0	26/1	3/1
A	**P122**	48	94	82	20123	246	6/0	67/0	154/4	8/4	5/1	3/0	0/0
A	**P205**	62	95	87	23215	629	24/1	237/7	344/9	14/1	5/0	7/0	3/0
A	**P317**	47	94	83	20790	291	10/0	94/1	161/5	7/0	11/0	7/0	3/0
A	**P348**	64	95	86	20859	323	15/1	108/2	173/6	11/5	10/3	4/0	0/1
A	**P378**	118	96	94	24070	423	14/2	123/1	241/5	17/7	16/4	4/0	1/0
A	**P386**	120	96	94	23534	396	17/3	108/4	205/11	23/4	21/1	10/1	3/0
A	**P398**	45	93	81	20310	316	13/0	88/1	207/0	3/1	4/2	6/0	2/0
A	**P425**	48	94	82	22601	707	20/1	265/4	383/7	17/2	8/2	12/0	4/0
A	**P506**	120	96	94	23452	430	18/3	121/1	215/9	42/4	23/1	8/0	4/1
B	**P217**	81	96	90	20429	260	8/0	72/0	173/0	4/0	4/0	5/0	2/0
B	**P306**	61	95	87	19925	437	10/0	128/0	276/1	9/2	10/1	8/0	1/0
B	**P351**	46	93	80	20411	246	8/1	72/2	159/3	7/3	4/0	4/0	0/0
B	**P367**	55	95	85	19262	263	15/0	77/0	165/0	9/0	5/0	6/0	0/0
B	**P388**	43	93	80	18084	228	10/0	66/1	148/2	4/0	1/1	3/0	1/0
B	**P462**	103	96	94	23686	503	23/3	139/9	281/8	25/7	19/3	4/0	2/0

	mean	70	95	86	21551	394	17	122	236	15	11	7	2
	%						4,1	29,7	57,6	3,7	2,6	1,8	0,5

Supplementary Table 3. Summary of loci (minimum lodscore threshold: 0,9 and length: >1Mb) identified in the P20 family. Identified intervals using the model of an autosomal dominant disorder and a summary of variants identified in the proband (Patient III.1) of the P20 family following exome sequencing.

INTERVAL	Size (Mb)	Total variations	Total variations (excluding snp>1%	Essential splicing	Synonymous	In frame del or dup	Non-synonymous	Frameshift	Stop gained	Start or stop lost
Whole genome		24058	613	38/2	135/9	3/0	398/12	7/0	26/1	3/1
linkage (treshold 0,9, Length 1Mb)	367,3	3015	77	7/1	19/1	2/0	50/0	1/0	1/0	1/0
Chr1 : 159986339-169066351	9,1	78	1	0/0	0/0	0/0	0/0	1/0	0/0	0/0
Chr1 : 201051582-203768328	2,7	61	1	0/0	1/0	0/0	0/0	0/0	0/0	0/0
Chr2 : 107252924-113009021	5,8	43	0	0/0	0/0	0/0	0/0	0/0	0/0	0/0
Chr2 : 113046185-157564814	44,5	193	7	2/0	1/0	0/0	5/0	0/0	0/0	0/0
Chr3 : 188043232-197315115	9,3	407	9	0/0	3/0	0/0	6/0	0/0	0/0	0/0
Chr4 : 140729346-145180928	4,5	21	0	0/0	0/0	0/0	0/0	0/0	0/0	0/0
Chr4 : 155640777-178501293	22,9	65	1	0/0	1/0	0/0	0/0	0/0	0/0	0/0
Chr5 : 233188-8790528	8,6	70	2	0/0	0/0	1/0	1/0	0/0	0/0	0/0
Chr5 : 115412737-175074644	59,7	361	12	0/0	5/0	0/0	7/0	0/0	0/0	0/0
Chr7 : 53285915-106106338	52,8	446	12	1/0	2/0	0/0	9/0	0/0	0/0	0/0
Chr7 : 156767585-159072828	2,3	14	0	0/0	0/0	0/0	0/0	0/0	0/0	0/0
Chr8 : 55912151-70493974	14,6	22	1	0/0	0/0	0/0	1/0	0/0	0/0	0/0
Chr9 : 122302024-133481912	11,2	144	6	1/0	1/0	0/0	4/0	0/0	1/0	0/0
Chr10 : 29499570-60265404	30,8	185	3	0/0	1/0	0/0	2/0	0/0	0/0	0/0

Chr10 : 78054402-91629054	13,6	89	1	0/0	0/0	0/0	1/0	0/0	0/0	0/0
Chr11 : 5451875-21393685	15,9	287	6	3/0	0/0	1/0	4/0	0/0	0/0	1/0
Chr11 : 126768090-134835614	8,2	44	3	0/0	1/0	0/0	2/0	0/0	0/0	0/0
Chr12 : 20158160-24098019	3,9	19	0	0/0	0/0	0/0	0/0	0/0	0/0	0/0
Chr14 : 72470336-94266671	21,8	156	6	0/0	2/0	0/0	4/0	0/0	0/0	0/0
Chr15 : 93589177-102162555	8,8	55	0	0/0	0/0	0/0	0/0	0/0	0/0	0/0
Chr18 : 14090993-23044024	9,0	47	0	0/0	0/0	0/0	0/0	0/0	0/0	0/0
Chr21 : 40448889-47874268	7,6	208	6	0/1	1/1	0/0	4/0	0/0	0/0	0/0

Supplementary Table 4. Summary of clinical and brain imaging phenotypes associated with mutations in *KIF5C, KIF2A, TUBG1* and *DYNC1H1* genes. SD: standard deviation; y: year; m: month; N: Normal; N/A: not available; SBH: subcortical band heterotopia; PMG: polymicrogyria; ID: intellectual disability; post: posterior.

Patient		**P20**	**P462**	**P147**	**P367**	**P388**	**P478**
Genetic	**Gene**	***KIF5C***	***KIF2A***	***KIF2A***	***TUBG1***	***TUBG1***	***TUBG1***
	Refseq	NM_004522.2	NM_001098511	NM_001098511	NM_001070	NM_001070	NM_001070
	cDNA	c.710A>T	c.961C>G	c.950G>A	c.1160T>C	c.275A>G	c.991A>C
	Protein	p.E237V	p.H321D	p.S317N	p.L387P	p.Y92C	p.T331P
	Transmission	Maternal mosaicism	*de novo*	*de novo*	*de novo*	*de novo*	Father DNA's unavailable
	Age at last evaluation	1 m	1 y	4 y	21 y	1.5 y	31 y
Clinic	**Head circumference**	Microcephaly (-4SD)	Microcephaly (-4SD)	Microcephaly (-2.5SD)	Microcephaly (-5.5 SD)	Microcephaly (-4SD)	Normocephaly
	Neurodevelopment	Bedridden	Bedridden	Bedridden	Bedridden	Bedridden	Moderate ID
	Neurological examination	Spastic tetraplegia	Spastic tetraplegia	Spastic tetraplegia	Spastic tetraplegia	Spastic tetraplegia	N/A
	Epilepsy	Early onset epilepsy	Early onset epilepsy	Early onset epilepsy	Early onset epilepsy	Infantile spasms	Early onset epilepsy
	Axonal Neuropathy	N	N/A	N/A	N	N	N/A
	Other signs	Arthrogryposis	IntraUterine Growth Retardation	Nystagmus			Cataract
MRI	**Cortex**	Frontal and perisylvian PMG	Frontal SBH and post. Pachygyria, Thick Cortex	Post. Agyria and frontal Pachygyria	Post. Agyria and frontal Pachygyria, Thick Cortex	Post. Agyria and frontal Pachygyria, Thick Cortex	Post. Pachygyria and post. SBH
	Basal ganglia	N	Dysmorphic	N	N	N	N
	Corpus callosum	Thin	Thin	Thin	Thin	Thick and dysmorphic	Thick and dysmorphic
	Brainstem	N	N	N	N	N	N
	Cerebellum	N	N	N	N	N	N

Patient		P144	P582	P122	P217	P398	P535
Genetic	**Gene**	***DYNC1H1***	***DYNC1H1***	***DYNC1H1***	***DYNC1H1***	***DYNC1H1***	***DYNC1H1***
	Refseq	NM_001376	NM_001376	NM_001376	NM_001376	NM_001376	NM_001376
	cDNA	c.del1976-1987	c.386A>T	c.10008G>T	c.10151G>A	c.4700G>A	c.10031G>A
	Protein	p.del659-662	p.K129I	p.K3336N	p.R3384Q	p.R1567Q	p.R3344Q
	Transmission	*De novo*	*de novo*	*de novo*	*de novo*	*de novo*	*de novo*
	Age at last evaluation	15 y	10 y	12 y	10 y	7 y	5 y
Clinic	**Head circumference**	Microcephaly (-2.5 SD)	Normocephaly	Microcephaly (-4 SD)	Microcephaly (-4 SD)	Normocephaly	Normocephaly
	Neurodevelopment	Bedridden	Severe ID	Bedridden	Bedridden	Severe ID	Severe ID - autistic features
	Neurological examination	Spastic tetraplegia	Normal	Spastic tetraplegia	Spastic tetraplegia	Normal	
	Epilepsy	Early onset epilepsy	Late onset epilepsy	Early onset epilepsy	Early onset epilepsy	Absent	Lennox Gastaut
	Axonal Neuropathy	N/A	N/A	Foot deformities	Foot deformities	Foot deformities	N/A
MRI	**Cortex**	Post. Pachygyria	Post. Pachygyria	Post. Pachygyria - Frontal PMG, Nodular Heterotopia	Post. Pachygyria - Frontal PMG	Frontal PMG	Post. Agyria, Nodular Heterotopia
	Basal ganglia	N	N	Dysmorphic	Dysmorphic	N	Dysmorphic
	Corpus callosum	Thin	Thick	Hypoplasic and Dysmorphic	Dysmorphic	N	Hypoplasic and dysmorphic
	Brainstem	N	N	Hypoplasic	Hypoplasic	N	N
	Cerebellum	N	N	Vermian Hypoplasia	Mild vermian Hypoplasia	N	N

Patient		360J	346D-1	346D-2	346D-mother	574C
Genetic	**Gene**	***DYNC1H1***	***DYNC1H1***	***DYNC1H1***	***DYNC1H1***	***DYNC1H1***
	Refseq	NM_001376	NM_001376	NM_001376	NM_001376	NM_001376
	cDNA	c.5884C>T	c.9722A>C	c.9722A>C	c.9722A>C	c.10031G>A
	Protein	p.R1962C	p.K3241T	p.K3241T	p.K3241T	p.R3344Q
	Transmission	*de novo*	Familial	Familial	Familial	*de novo*
	Age at last evaluation	19 y	11 y	8 y	39 y	3 y
Clinic	**Head circumference**	Normocephaly	Normocephaly	Normocephaly	Normocephaly	25%
	Neurodevelopment	Severe ID	Normal	Mild ID	Normal	Moderate ID
	Neurological examination	Awkwardness	Normal	Awkwardness	Normal	Awkwardness
	Epilepsy	Focal seizures from age 2 m to 8 y	Focal seizures since the age of 2 y 5 m	Focal seizures since the age of 1 y 2 m	Focal epilepsy since the age of 10 y	Focal seizures since the age of 5 m
	Axonal Neuropathy	N	N	N	N	N
MRI	**Cortex**	Predominent post. pachygyria	Post. Pachygyria	Post. Pachygyria	Post. Pachygyria	Predominent post. pachygyria
	Basal ganglia	N	N	N	N	N
	Corpus callosum	N	N	N	N	N
	Brainstem	N	N	N	N	N
	Cerebellum	N	N	N	N	Small vermis

Supplementary Table 5. Summary of Grantham, PolyPhen and Sift scores[8-10] for the identified *KIF5C, KIF2A, TUBG1* and *DYNC1H1* mutations.

Gene	refseq	cDNA	protein	Grantham Score		PolyPhen Score		Sift Score	
KIF5C	NM_004522.2	c.710A>T	p.E237V	121	radical	1,000	Probably Damaging	0,00	Affect Function
KIF2A	NM_001098511	c.961C>G	p.H321D	81	nonconservative	0,963	Probably Damaging	0,02	Affect Function
KIF2A	NM_001098511	c.950G>A	p.S317N	46	conservative	0,996	Probably Damaging	0,00	Affect Function
TUBG1	NM_001070	c.1160T>C	p.L387P	98	nonconservative	1,000	Probably Damaging	0,00	Affect Function
TUBG1	NM_001070	c.275A>G	p.Y92C	194	radical	1,000	Probably Damaging	0,01	Affect Function
TUBG1	NM_001070	c.991A>C	p.T331P	38	conservative	0,989	Probably Damaging	0,06	Tolerated
DYNC1H1	NM_001376	c.del1976-1987	p.del659-662	-	radical	-	Probably Damaging	-	-
DYNC1H1	NM_001376	c.386A>T	p.K129I	102	radical	1,000	Probably Damaging	0,13	Tolerated
DYNC1H1	NM_001376	c.10008G>T	p.K3336N	94	nonconservative	0,998	Probably Damaging	0,07	Tolerated
DYNC1H1	NM_001376	c.10151G>A	p.R3384Q	43	conservative	0,994	Probably Damaging	0,22	Tolerated
DYNC1H1	NM_001376	c.4700G>A	p.R1567Q	43	conservative	1,000	Probably Damaging	0,03	Affect Function
DYNC1H1	NM_001376	c.10031G>A	p.R3344Q	43	conservative	0,817	Potentially Damaging	0,45	Tolerated
DYNC1H1	NM_001376	c.5884C>T	p.R1962C	180	radical	1,000	Probably Damaging	0,00	Affect Function
DYNC1H1	NM_001376	c.9722A>C	p.K3241T	78	nonconservative	0,863	Potentially Damaging	0,04	Affect Function
DYNC1H1	NM_001376	c.10031G>A	p.R3344Q	43	conservative	0,817	Potentially Damaging	0,45	Tolerated

Supplementary Table 6. Number, length and dynamics of Bik1p-GFP labeled astral MTs. In this table G1 MTs were visualized with a Bik1p-GFP fusion in diploid cells. Results are average values ± s.e.m. Values in parentheses are the number of events, except for life-time in which the values in parentheses are the number of MTs. Growing, shortening and pause duration are in minutes. *** $p<0.001$, non parametric Mann and Whitney test comparisons of mutant cells vs. WT cells.

Strain	Growth rate Shortening rate μm / min	Catastrophe frequency Rescue frequency Events / sec	Growing duration Shortening duration Pausing duration	Lifetime sec
WT	0.74 +/- 0.0001 (54) 0.74 +/- 0.0001 (44)	0.023 +/- 0.003 (34) 0.033 +/- 0.003 (30)	0.44 +/- 0.04 (54) 0.28 +/- 0.02 (44) 0.23 +/- 0.02 (18)	73.4 +/- 6.4 (38)
p.W92C	0.77 +/- 0.01 (64) 0.75 +/- 0.1 (52)	0.022 +/- 0.004 (43) 0.023 +/- 0.005 (39)	0.49 +/- 0.05 (64) 0.39 +/- 0.04 (52) 0.21 +/- 0.02 (22)	101.3 +/- 11.7 (37)
p.V387P	0.75 +/- 0.0001 (63) 0.75 +/- 0.0001 (56)	0.025 +/- 0.004 (52) 0.023 +/- 0.004 (43)	0.42 +/- 0.03 (63) 0.34 +/- 0.03 (56) 0.26 +/- 0.03 (38)	121 +/- 12.2 (30) ***

Supplementary Table 7. MT Assembly rate, number and length of Bik1p-GFP labeled astral and spindle microtubules. Astral microtubules were examined in G1 cells. The frequency at which new MTs appeared at the SPBs (wt, n=10 cells; p.W92C, n= 15 cells; p.V387P, n=14 cells) is shown. Number, length and maximal mean were wt, n=38 MTs; W92C, n= 37 MTs; V387P, n=30 MTs). § Number of new MTs (resulting from either nucleation or regrowth) visible in the region of the SPBs per unit time. *** $p<0.001$, t test comparisons of mutant cells vs. WT cells.

Strain	MTs Assembled§ Per minute	MT number Per cell	MT length µm	Mean Max length µm
WT	1.42 +/- 0.11	2.3 +/- 0.09	2.2 +/- 0.14	3.1 +/- 0.19
p.W92C	0.5 +/- 0.07***	3.4 +/- 0.11***	3.3 +/- 0.25***	4.8 +/- 0.33***
p.V387P	1.15 +/- 0.08	2.5 +/- 0.07	2.4 +/- 0.15	3.3 +/- 0.19

Supplementary Table 8. Summary of patient phenotypes associated with *de novo* mutations in candidate genes encoding proteins with no apparent relation to the centrosome or to MTs. Note that for 4 patients (317, 348, 306 and 351), no relevant mutations were identified, but inherited variants were found in the following genes: *KIF20B, KIF26A, KIF9* (P317); *KIF9, DNAH3* (P348); *DNAH9, MCPH1* (P306); *DNAH5* (P351). ID: intellectual disability; PMG: polymicrogyria**.**

Group	Patient	Cortical Malformation Group	ID	Epilepsy	Other symptoms	Mutated candidate gene	Mutation (cDNA; protein)	Transmission	(Previously reported Associated disorder; OMIM)
A	**P205**	Asymetric PMG	Moderate	No seizure	Spastic Hemiplegy	*ZNF674*	c.601C>T; p.R201X	X-linked gene. Inherited from the mother	Mental retardation, X-linked; 300573
A	**P317**	BiFrontoParietal PMG	Severe Encephalopathy	Early onset seizure	Microcephaly	No			
A	**P348**	Perisylvian PMG	Moderate	No seizure	Spastic diplegia	No			
A	**P378**	Diffuse PMG	Severe Encephalopathy	Early onset seizure		*GRIN1*	c.1975C>T; p.R659W	*de novo*	Mental retardation, autosomal dominant, 138249
						CHRNB2	c.71G>A; p.W24X	*de novo*	Epilepsy, nocturnal frontal lobe; 118507
A	**P386**	Diffuse PMG	Severe Encephalopathy	No seizure	Swallowing difficulties	*TBC1D22B*	c.1297G>T; p.E433X	*de novo*	None
A	**P425**	Gyral simplification	Severe Encephalopathy	No seizure	Microphtalmy	*SOX2*	c.480C>G; p.Y160X	*de novo*	Optic nerve hypoplasia and abnormalities of the central nervous system; 184429
A	**P506**	Perisylvian PMG	Severe	Neonatal seizures		*SCN2A*	c.4782G>T; p.W1594C	*de novo*	Epileptic encephalopathy
						RAI1	c.2564T>C; p.L855P	*de novo*	Syndromic mental retardation (Smith-Magenis syndrome); 182390
B	**P306**	LIS-Post. Agyria	Severe Encephalopathy	Early onset seizure	Foot deformities	No			
B	**P351**	LIS-Post. Agyria	Severe	Early onset seizure		No			

1. Tian, G., Vainberg, I.E., Tap, W.D., Lewis, S.A. & Cowan, N.J. Specificity in chaperonin-mediated protein folding. *Nature* 375, 250-3 (1995).
2. Straight, A.F., Marshall, W.F., Sedat, J.W. & Murray, A.W. Mitosis in living budding yeast: anaphase A but no metaphase plate. *Science* 277, 574-8 (1997).
3. Carminati, J.L. & Stearns, T. Microtubules orient the mitotic spindle in yeast through dynein-dependent interactions with the cell cortex. *J Cell Biol* 138, 629-41 (1997).
4. Lin, H. et al. Polyploids require Bik1 for kinetochore-microtubule attachment. *J Cell Biol* 155, 1173-84 (2001).
5. Yamada, M. et al. LIS1 and NDEL1 coordinate the plus-end-directed transport of cytoplasmic dynein. *Embo J* 27, 2471-83 (2008).
6. Liu, J.S. et al. Molecular basis for specific regulation of neuronal Kinesin-3 motors by doublecortin family proteins. *Mol Cell* 47, 707-21 (2012).
7. Barkovich, A.J., Guerrini, R., Kuzniecky, R.I., Jackson, G.D. & Dobyns, W.B. A developmental and genetic classification for malformations of cortical development: update 2012. *Brain : a journal of neurology* 135, 1348-69 (2012).
8. Grantham, R. Amino acid difference formula to help explain protein evolution. *Science* 185, 862-4 (1974).
9. Kumar, P., Henikoff, S. & Ng, P.C. Predicting the effects of coding non-synonymous variants on protein function using the SIFT algorithm. *Nat Protoc* 4, 1073-81 (2009).
10. Ramensky, V., Bork, P. & Sunyaev, S. Human non-synonymous SNPs: server and survey. *Nucleic Acids Res* 30, 3894-900 (2002).